

1 **Heterochronic shifts in germband movements contribute to**
2 **the rapid embryonic development of the coffin fly *Megaselia***
3 ***scalaris***

4
5 Karl R. Wotton

6
7 EMBL/CRG Research Unit in Systems Biology, Centre for Genomic Regulation
8 (CRG), and Universitat Pompeu Fabra (UPF), Dr. Aiguader 88, 08003 Barcelona,
9 Spain

10 **Abstract**

11 The coffin fly, *Megaselia scalaris*, is a species of medical and forensic importance
12 and is increasingly being used for the study of genetics. Postmortem interval can be
13 estimated based on the life stage of *M. scalaris* recovered from corpses, therefore
14 many studies have addressed the duration of each life stage. These studies
15 demonstrate that embryogenesis completes significantly faster in *M. scalaris* than in
16 the congener *Megaselia abdita* and faster even than the 24 hours needed for
17 *Drosophila melanogaster* embryogenesis. However, until now it has been unclear if
18 this increased speed is achieved by reducing developmental time across all
19 embryonic stages or by the acceleration of individual stages and processes.
20 Furthermore, the large difference in developmental time between the *Megaselia*
21 species suggests that the staging scheme developed for *M. abdita* will not be directly
22 applicable to *M. scalaris*. Here I use time-lapse imaging to create a staging scheme
23 for *M. scalaris* embryogenesis. Comparison of stages between *D. melanogaster* and
24 both *Megaselia* species reveals heterochronic shifts, increased coordination of
25 morphogenetic movements and compression of individual stages all contribute to the
26 rapid development of *M. scalaris*.

27
28
29
30
31 **Abbreviations**

32 TED: percentage of total embryonic development

33 AEL: time after egg laying

34 **1. Introduction**

35 *Megaselia scalaris* (Loew, 1866) is a fly in the family Phoridae, also referred to as the
36 hump-backed or the scuttle flies. Its ability to reach buried carrion has lead to its use
37 in forensics and is reflected in another alternative name, the coffin fly. This name has
38 the benefit of distinguishing it from *Megaselia abdita*, also referred to as the scuttle fly.
39 In addition to its use in estimating postmortem interval in forsensics, *M. scalaris* is of
40 medical important due to the ability of its larvae to invade living tissues causing
41 myiasis (see Disney, 2008; Varney and Noor, 2010 for reviews of *M. scalaris* biology).

42 The genus *Megaselia* forms one of the largest groups among the phorids (one of the
43 earliest branching lineage in the radiation of the cyclorrhaphan flies; see Jiménez-
44 Guri et al., 2013; Wiegmann et al., 2011) and both *M. abdita* and *M. scalaris* have
45 emerged as useful models for genetics. In the case of *M. scalaris*, this has mostly
46 focused on sex determination (Sievert et al., 1997; Traut, 2010, 1994; Willhoeft and
47 Traut, 1995, 1990), while the focus with *M. abdita* has been on embryonic
48 development (Lemke et al., 2008; Rafiqi et al., 2008; Stauber et al., 2008, 2000,
49 1999; Wotton et al., 2014).

50 Genomic resources exist for both species, with a transcriptome available for *M.*
51 *abdita* (Jiménez-Guri et al., 2013; <http://diptex.crg.es/>) and a genome available for *M.*
52 *scalaris* (Rasmussen and Noor, 2009;
53 http://metazoa.ensembl.org/Megaselia_scalaris). Additionally, techniques developed
54 for *M. abdita*, including in situ hybridisation (Wotton et al., 2014, 2012) and gene
55 knock-down (Rafiqi et al., 2013a, 2013b, 2013c) are likely to be directly applicable to
56 *M. scalaris*.

57 Numerous publications have addressed the duration of *M. scalaris* development at
58 different temperatures (see Table 1 in Disney, 2008) with egg to adult taking 17.2-

59 18.4 days at 25°C, of which around 17 hours were needed for embryonic
60 development (Prawirodisastro and Benjamin, 1979). Embryonic development in *M.*
61 *abdita* lasts significantly longer than this, at least 24 hours (as in *D. Melanogaster*)
62 and up to around 27.5 hours under oil (Rafiqi et al., 2013a; Wotton et al., 2014).
63 However, no systematic characterisation and analysis of *M. scalaris* embryonic
64 development has been carried out. To investigate whether this reduced
65 developmental time is the result of a global decrease in developmental time at each
66 embryonic stage or a reduction in individual stages or events, I carried out a detailed
67 description of embryonic development. Stages were homologised to *D. melanogaster*
68 and *M. abdita* development. Comparison of stages across all 3 species reveals a
69 heterochronic shift in the stage in which the germband reaches its maximum extent
70 that leads to the earlier completion of germband retraction in *M. scalaris*. Additionally,
71 increased coordination of the morphogenetic movements of head involution and
72 dorsal closure, as compared to *M. abdita*, combine with the altered germband
73 dynamics to result in a compression of the time needed to complete stages 9 through
74 13 (from transient segmentation to the beginning of head involution). Additional
75 heterochronic shifts of serosal rupture and contraction to an earlier stage, as
76 compared to *M. abdita*, mean that *M. Scalaris* is enclosed in extraembryonic tissue
77 for substantially less time than is *M. abdita*. A heterochronic shift is also found in the
78 timing at which the ventral nervous system begins to shorten, from stage 16 in *D.*
79 *melanogaster* and stage 15 in *M. abdita* to stage 14 in *M. scalaris*. Finally, both
80 *Megaselia* species show a reduction in the time needed to complete stage 16 (from
81 the appearance of intersegmental grooves at mid-dorsal levels until the dorsal ridge
82 overgrows clypeolabrum).

83

84

85 **2. Materials and Methods**

86 **2.1 Fly culture and embryo collection**

87 *M. scalaris* embryos were collected after 5–10 min laying time, and dechorionated for
88 1 min 20 sec in 25% bleach. To image the embryos I brushed the dechorionated
89 embryos onto a microscopy slide and covered them with a drop of 10S Voltalef oil
90 ensuring that the embryos did not dry out.

91 **2.2 Time-lapse imaging**

92 Slides were placed on a temperature-controlled platform at 25°C, and embryos were
93 imaged with a Leica DM6000B upright compound microscope using a 20x objective,
94 and time intervals between image acquisitions of every 1 min. Specifications of
95 embryo orientation for each time-lapse are provided in Supporting File S1. Movies
96 were processed using ImageJ (<http://rsbweb.nih.gov/ij>).

97 **3. Results & Discussion**

98 **3.1 Embryonic staging scheme for *M. scalaris* development**

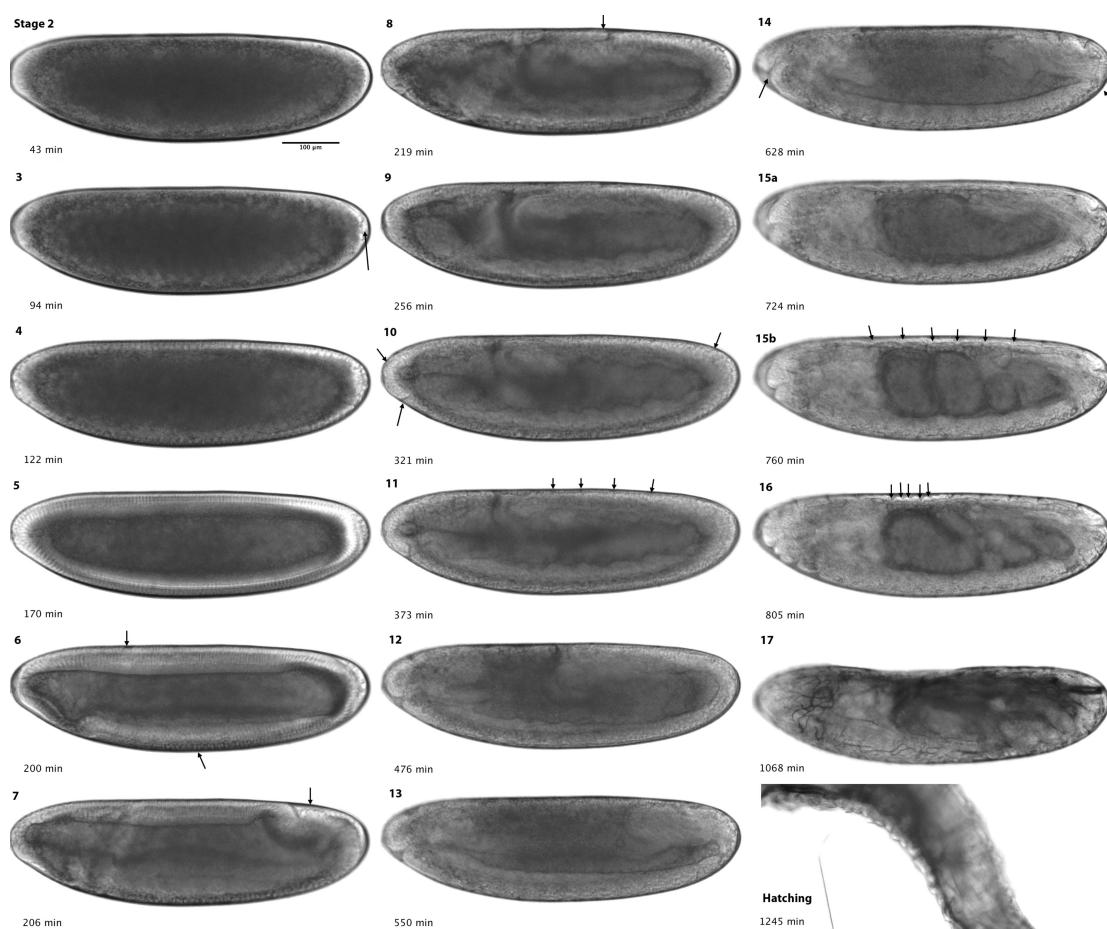
99 Embryos were collected shortly after egg laying, dechorinated and placed on a
100 microscope slide under Voltalef oil. Live imaging with differential interference contrast
101 (DIC) was used to produce a series of movies covering all stages of embryonic
102 development (see Supporting Movie S1). At 25°C and under voltalef oil
103 embryogenesis lasts approximately 22 hours (hrs) from oviposition until hatching, 2
104 hours shorter than in *D. melanogaster* and approximately 5 hrs 30 min shorter than in
105 the congener *M. abdita*.

106 Development can be divided into 17 stages roughly corresponding to Bownes' stages
107 in *D. melanogaster* and *M. abdita* (Campos-Ortega and Hartenstein, 1997; Wotton et
108 al., 2014). Each stage can be distinguished by distinct morphological markers, as

109 shown in Figure 1 (also see Supporting Movie S1). The similarity between

110 *D. melanogaster*, *M. abdita* and *M. scalaris* development allows a direct comparison
111 between developmental stages, as discussed below and shown in Table 1 and
112 Figure 2 (see section 3.2).

113 In this section, I provide an overview over all stages of development and provide a
114 comparison to the well characterised embryology of *D. melanogaster* (Campos-
115 Ortega and Hartenstein, 1997). All times are displayed as hrs:min unless otherwise
116 indicated. Raw data for each event including the number of embryos examined (*n*)
117 and standard deviations (SDs) are supplied in Supporting File S1. To assist
118 identification of stages under different conditions (i.e. not under oil), and at different
119 temperatures, a percentage of total embryonic development (TED) is supplied.



120

121 **Figure 1. Embryonic staging and developmental events in *M. scalaris*.** Embryos
122 are shown as lateral views: anterior is to the left, dorsal is up. Stage numbers

123 (roughly corresponding to Bownes' stages in *D. melanogaster*) are shown at the top
124 left, and time after egg laying (AEL) in minutes in the bottom left corner of each panel.
125 Black arrows indicate morphological landmarks. See main text for a detailed
126 description, and Figure 2 and Table 1 for comparative timing of stages with reference
127 to *D. melanogaster* and *M. abdita*.

128
129 **Stage 1:** 0:00–0:20 (duration: 0:20, 1.5% TED). This stage begins at egg laying, and
130 lasts until the end of the first two cleavage divisions, at the beginning of
131 cleavage cycle 3 (C3). The number of cleavage cycles appears to be conserved
132 within the Diptera with *D. melanogaster*, *M. abdita* and *C. albipunctata* all undergoing
133 14 cleavage cycles before gastrulation (Foe and Alberts, 1983; Jimenez-Guri et al.,
134 2014), I therefore base the timings for *M. scalaris* development on this observation.
135 Since all cleavage cycles up to C12 are of a very similar duration (approximately 10
136 min), we infer stage 1 to last for at least 20 min. All 'times after egg laying (AEL)'
137 below include a correction based on this estimate (see Supporting File S1 for raw
138 timing data, and time adjustment values). In *D. melanogaster*, stage 1 occurs over a
139 25 min period (1.4% TED) (Campos-Ortega and Hartenstein, 1997 and references to
140 *D. melanogaster* development hereafter unless stated).

141 **Stage 2:** 0:20–1:28 (duration: 1:08, 5.2% TED). Cleavage cycles C3 to C8 take place.
142 During this time, an empty space appears between the vitelline membrane and the
143 egg cytoplasm at the anterior and posterior poles. In *D. melanogaster*, stage 2 occurs
144 from 0:25–1:05 and takes 0:40 (3% TED).

145 **Stage 3:** 1:28–1:38 (duration: 0:10, 0.8% TED). Stage 3 includes cleavage cycle C9
146 and the beginning of C10. At this stage, nuclei divide and migrate outwards, and the
147 pole buds form (Figure 1, stage 3, black arrow). Stage 3 ends with the arrival of
148 nuclei at the periphery of the embryo. In *D. melanogaster*, this stage occurs from

149 1:05–1:20 and lasts for 0:15 (1% TED). During this stage, the empty space at the
150 posterior of the embryo disappears in both species. The duration of blastoderm
151 cleavage cycle 10 for *D. melanogaster*, *M. abdita* and *M. scalaris* is around 9, 13 and
152 13 min respectively.

153 **Stage 4:** 1:38–2:39 (duration: 0:61, 4.7% TED). At the onset of this stage, the nuclei
154 have reached the periphery and form the syncytial blastoderm, cleavage cycles 11 to
155 13 take place. Stage 4 terminates at the beginning of cleavage cycle C14. In
156 *D. melanogaster*, the syncytial blastoderm stage occurs from 1:20–2:10 and lasts for
157 0:50 (3.5% TED). The duration of blastoderm cleavage cycles 11-13 for *D.*
158 *melanogaster*, are around 10, 12 and 21 mins, for *M. abdita*: 11, 14 and 23 mins, and
159 for *M. scalaris*: 12, 12 and 20 mins respectively.

160 **Stage 5:** 2:39–3:19 (duration: 0:40, 3% TED). Similar to previous blastoderm cycles,
161 cellular membranes begin to form at cleavage cycle C14, but these now
162 progressively grow to engulf the elongating blastoderm nuclei forming the cellular
163 blastoderm. Nuclear morphology changes from circular to elongated. Stage 5 ends
164 just before the onset of gastrulation, and is marked by the wavy appearance of the
165 ventral blastoderm cells (seen as uneven apical and basal surfaces), and the slight
166 dorsal movement of the pole cells. In *D. melanogaster*, this stage occurs from 2:10–
167 2:50 and lasts for 0:40 (3% TED).

168 **Stage 6:** 3:19–3:27 (duration: 0:08, 0.6% TED). Early gastrulation events occur: the
169 ventral and cephalic furrows form (Figure 1, stage 6, black arrows), and the pole cells
170 continue to shift dorsally. Stage 6 ends when the cell plate carrying the pole cells
171 reaches a horizontal position. In *D. melanogaster*, this stage occurs from 2:50–3:00
172 and lasts for 0:10 (1% TED).

173 **Stage 7:** 3:27–3:32 (duration: 0:05, 0.4% TED). This stage begins with the pole cell
174 plate in a horizontal position (parallel to the A–P axis; Figure 1, stage 7, black arrow).

175 The plate continues to tilt, forming a pocket (the amnioproctodeal invagination). The
176 beginning of cephalad (headwards) movement of this invagination marks the end of
177 stage 7. The dorsal folds and amnioproctodeal invagination are less conspicuous in
178 both *M. scalaris* and *M. abdita* movies. In *D. melanogaster*, this stage occurs from
179 3:00–3:10 and lasts for 0:10 (1% TED).

180 **Stage 8:** 3:32–4:39 (duration: 1:07, 5.1% TED). This stage starts with the cephalad
181 movement of the amnioproctodeal invagination, marking the onset of the rapid phase
182 of germband extension. The germband reaches approximately 40% A–P position
183 (0% A–P position is at the anterior pole), and the amnioserosal lip forms (Figure 1,
184 stage 8, black arrow). Originating from this lip, the serosa migrates to eventually
185 engulf the entire embryo at stage 11 as is seen in *M. abdita*. Interestingly this stage
186 lasts longer in both *Megaselia* species than in *D. melanogaster*. Stage 8 ends with
187 the transient appearance of mesodermal segmentation. In *D. melanogaster*, this
188 stage occurs from 3:10–3:40 and lasts for 0:30 (2% TED). During this time, the
189 germband reaches beyond 40% A–P position. On the other hand, no serosal
190 migration occurs in *D. melanogaster* since extraembryonic tissues are reduced to a
191 dorsal amnioserosa that does not evaginate or migrate.

192 **Stage 9:** 4:39–5:07 (duration: 0:28, 2.1% TED). The germband continues to extend
193 but at a slower rate (slow phase of germband extension), and the serosa continues to
194 migrate ventrally. Also at this stage, and unlike in *D. melanogaster* and *M. abdita*
195 where it occurs at stage 10, the germband reaches its maximum extent, around 30%
196 A–P position. Stage 9 ends with the formation of the stomodeal invagination (seen
197 more clearly in Figure 1, stage 10, ventral-anterior black arrow). In *D. melanogaster*,
198 this stage occurs from 3:40–4:20 and lasts for 0:40 (3% TED).

199 **Stage 10:** 5:07–6:05 (duration: 0:58, 4.4% TED) During this stage, the stomodeum
200 continues to form (Figure 1, stage 10, ventral-anterior black arrow). Stage 10 ends

201 with the appearance of parasegmental furrows (seen more clearly in Figure 1,
202 stage 11, dorsal black arrows). During this time, the serosa continues to migrate
203 (Figure 1, stage 10, dorso-lateral black arrows). In *D. melanogaster*, this stage
204 occurs from 4:20–5:20 and lasts for 1:00 (4% TED), during which the germband
205 reaches its maximum extent at 25% A–P position.

206 **Stage 11:** 6:05–6:48 (duration: 0:43, 3.3% TED). Stage 11 begins with the
207 appearance of parasegmental furrows (Figure 1, stage 11, dorsal black arrows), and
208 ends with the beginning of germband retraction. During this time the serosa fuses
209 forming a complete extraembryonic layer around the embryo. The serosa remains
210 intact for around 4.5 hrs before finally breaking at stage 14. In contrast, this extra
211 embryonic layer persists for around 7 hrs in *M. abdita* and consequently does not
212 break until stage 15. In *D. melanogaster*, this stage occurs from 5:20–7:20 and lasts
213 for 2:00 (8% TED).

214 **Stage 12:** 6:48–8:54 (duration: 2:06, 9.6% TED). During this stage, the germband
215 retracts. Stage 12 ends with the completion of this process. In *D. melanogaster*, this
216 stage occurs from 7:20–9:20 and lasts for 2:00 (8% TED).

217 **Stage 13:** 8:54–9:18 (duration: 0:24, 1.8% TED). Stage 13 lasts from the completion
218 of germband retraction until the onset of head involution. During this time, the dorsal
219 opening of the embryo remains covered by the amnion, and the serosa envelopes
220 the entire embryo. Dorsal closure starts at the same time as the lengthening of the
221 gut. In *D. melanogaster*, this stage occurs from 9:20–10:20 and lasts for 1:00 (4%
222 TED), during which the dorsal egg surface remains open and the dorsal hole is
223 covered by the amnioserosa.

224 **Stage 14:** 9:18–11:08 (duration: 1:50, 8.4% TED). Stage 14 starts at the beginning of
225 head involution, and ends with closure of the midgut. During this time, the serosa
226 ruptures (10:40) at a ventro-posterior position, slightly more pole-ward than in *M.*

227 *abdita* and one stage earlier (Figure 1, stage 14, black arrow at posterior pole).
228 During its retraction, the serosa first rounds the posterior pole before rounding the
229 anterior pole, to be contracted into the dorsal hole 40 min after snapping (retraction
230 also takes 40 min in *M. abdita*). Additionally during this stage, the ventral nerve cord
231 (VNC) starts to shorten. In contrast, this occurs during stage 15 in *M. abdita* and at
232 stage 16 in *D. melanogaster*. The head continues to involute beyond the end of this
233 stage (Figure 1, stage 14, black arrow at anterior pole), and this process completes
234 only by the time the serosa ruptures at stage 15. In *D. melanogaster*, stage 14 occurs
235 from 10:20–11:20 and lasts for 1:00 (1.4% TED).

236 **Stage 15:** 11:08–13:25 (duration: 2:17, 10.4% TED). Stage 15 starts at the closure of
237 the midgut (Figure 1, stage 15a), and covers the completion of dorsal closure and
238 dorsal epidermal segmentation. This stage ends when intersegmental grooves can
239 be distinguished at mid-dorsal levels (Figure 1, stage 15b, black arrows). Dorsal
240 closure completes and dorsal epidermal segmentation is visible. Also during this
241 stage, the gut constricts, and muscle contractions begin. In *D. melanogaster*, this
242 stage occurs from 11:20–13:00 and lasts for 1:40 (7% TED).

243 **Stage 16:** 13.25–13:44 (duration: 0:19, 1.5% TED). Stage 16 begins with the
244 appearance of the lateral intersegmental grooves (Figure 1, stage 16, black arrows),
245 and ends when the dorsal ridge has completely overgrown the tip of the
246 clypeolabrum (completion of head involution). The VNC continues to shorten;
247 completion of this movement is not clearly detectable and probably continues into
248 stage 17. In *D. melanogaster*, this stage occurs from 13:00–16:00 and lasts for 3:00
249 (13% TED).

250 **Stage 17:** 13:44–21:53 (duration: 8:09, 37% TED). During this stage, the retraction of
251 the VNC is likely to continue and reach completion. The trachea fill with air at around

252 18 hrs AEL. The first instar larva hatches at around 22 hrs AEL. In *D. melanogaster*,
253 this stage occurs from 16:00–24:00 and lasts for 8:00 hrs (33% TED).

254

255 **3.2 Comparative analysis of embryonic development in *M. scalaris*, *M.***
256 ***abdita* and *D. melanogaster***

257 *M. scalaris* embryonic development completes approximately 2 hrs faster than in *D.*
258 *melanogaster* and 5.5 hrs faster than in the congener *M. abdita*. A comparative
259 overview of embryonic development between *D. melanogaster*, *M. abdita* and
260 *M. scalaris* is shown in Figure 2, while stage durations and %TED values are shown
261 in Table 1. Using these resources I next discuss the features of *M. scalaris* that may
262 account for the decreased time needed for embryonic development.

263 The timing of stages 1 to 7 is remarkably similar in all 3 species. At the start of stage
264 7 (when the pole cell plate reaches a horizontal position) only 30 min separates *D.*
265 *melanogaster* (at 3 hrs AEL) from *M. scalaris*, and 45 min from *M. abdita*.

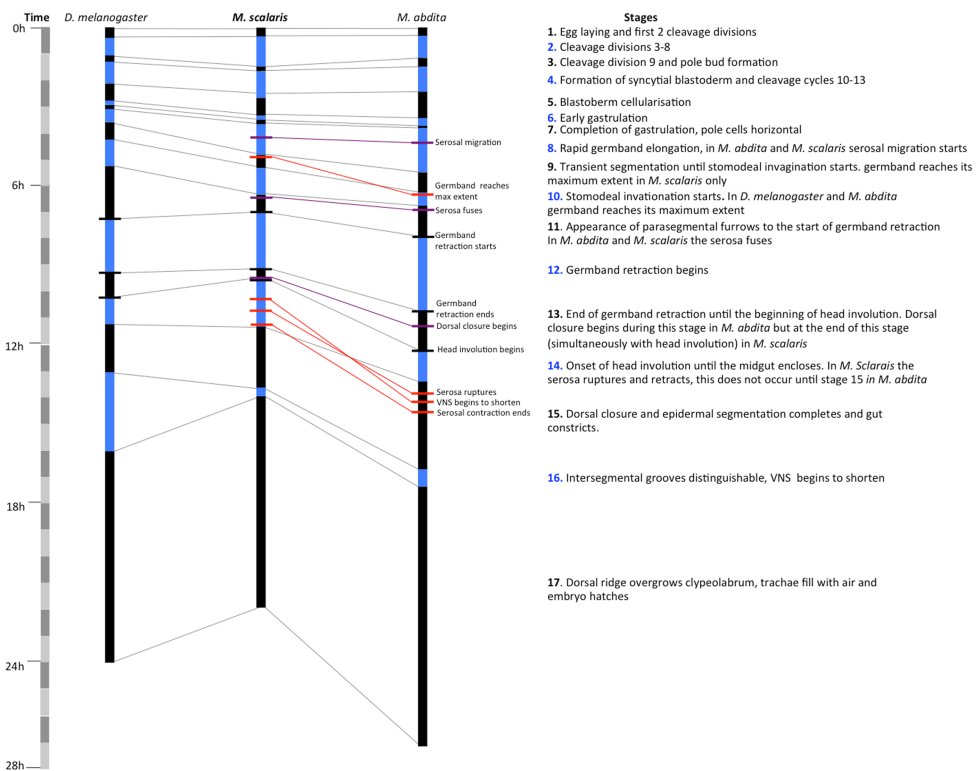
266 At stage 8 serosal migration begins in both *Megaselia* species but is absent from *D.*
267 *melanogaster*. This may explain the shorter time needed to complete stage 8 in *D.*
268 *melanogaster* (30 min), while this stage takes around 40 min longer in *M. scalaris*
269 and 1 hr 10 min longer in *M. abdita*.

270 At stage 9 the germband of *M. scalaris* reaches its maximum extent, one stage
271 earlier than in the other species (Campos-Ortega and Hartenstein, 1997; Wotton et
272 al., 2014). This represents a large heterochronic shift and consequently the time at
273 which the germband retracts (at stage 12) starts around 1 hr 20 min before it occurs
274 in *M. abdita*. Additionally, germband retraction is completed as quickly in *M. scalaris*
275 as in *D. melanogaster*, around 50 min quicker than in *M. abdita*. These features of
276 germband extension create a relatively short stage 11 (30 min shorter than in *M.*

277 *abdita* and 1 hr 17 min shorter than in *D. melanogaster*) and consequently *M. scalaris*
278 reaches the end of stage 11 before *D. melanogaster*. Stage 12 lasts for around 2 hrs
279 in both *D. melanogaster* and *M. scalaris* but continues for an additional 50 min in *M.*
280 *abdita*. At stage 13, in *M. scalaris*, dorsal closure and head involution occur
281 simultaneously (in *M. abdita*, the start of head involution occurs approximately 1 hour
282 after dorsal closure begins) and this, together with the altered germband dynamics,
283 forms a shorter stage 13 than in the other species. Therefore *M. scalaris* remains
284 ahead in development until the end of stage 13.

285 A further heterochronic shift in *M. scalaris* sees the shortening of the VNS beginning
286 at stage 14, a stage earlier than in *M. abdita* (stage 15), and 2 stages earlier than in
287 *D. melanogaster* (stage 16). Additionally, at this stage the serosa ruptures and is
288 contracted into the dorsal hole one stage earlier than in *M. abdita*. The
289 disappearance of the serosa is correlated with a lengthened stage 14 in *M. scalaris*
290 (50 min more than in *D. melanogaster* and 34 min more than in *M. abdita*) and a
291 lengthened stage 15 in *M. abdita*.

292 Stage 16 is significantly shorter in both *Megaselia* species than in *D. melanogaster* (2
293 hrs 40 min shorter in *M. scalaris*) and allows *M. scalaris* to begin stage 17 around 2
294 hrs 16 min before *D. melanogaster*, and around 4 hrs before *M. abdita* starts. Finally,
295 stage 17 ends embryonic development and takes around 8 hrs in both *M. scalaris*
296 and *D. melanogaster* while *M. abdita* requires a further 2 hrs before hatching.



297

298 **Figure 2. Comparative timing of embryonic developmental stages in**
 299 ***D. melanogaster*, *M. scalaris* and *M. abdita*.** The duration of each stage is shown
 300 for each species in alternating black and blue bars. The time scale is divided into
 301 blocks of 1 hr on the far left hand side. A brief description of each stage is given on
 302 the right. Landmarks of development are indicated to the right of the *M. abdita* time
 303 scale and discussed in the text. Red horizontal bars indicate heterochronic shifts
 304 between *M. abdita* and *M. scalaris*, purple bars indicate landmark events occurring
 305 during a stage, while black bars indicate landmark events occurring at stage
 306 boundaries.

307

308

309

310

311

312

| Stage | <i>D. melanogaster</i> (Campos-Ortega and Hartenstein, 1997) | | <i>M. abdita</i> (Wotton et al., 2014) | | <i>M. scalaris</i> | |
|-------|---|------|---|------|--------------------|-------|
| | Stage duration | %TED | Stage duration | %TED | Stage duration | %TED |
| 1 | 0:25 | 1.4 | 0:20 | 1.2 | 0:20 | 1.5 |
| 2 | 0:40 | 3 | 0:50 | 3 | 1:08 | 5.2 |
| 3 | 0:15 | 1 | 0:23 | 1.4 | 0:10 | 0.8 |
| 4 | 0:50 | 3.5 | 0:57 | 3.4 | 1:01 | 4.7 |
| 5 | 0:40 | 3 | 0:58 | 4 | 0:40 | 3.0 |
| 6 | 0:10 | 1 | 0:18 | 1 | 0:08 | 0.6 |
| 7 | 0:10 | 1 | 0:05 | 0.3 | 0:05 | 0.4 |
| 8 | 0:30 | 2 | 1:38 | 6 | 1:07 | 5.1 |
| 9 | 0:40 | 3 | 0:47 | 3 | 0:28 | 2.1 |
| 10 | 1:00 | 4 | 0:33 | 2 | 0:58 | 4.4 |
| 11 | 2:00 | 8 | 1:13 | 4 | 0:43 | 3.3 |
| 12 | 2:00 | 8 | 2:51 | 10 | 2:06 | 9.6 |
| 13 | 1:00 | 4 | 1:26 | 5.2 | 0:24 | 1.8 |
| 14 | 1:00 | 4 | 1:14 | 4 | 1:50 | 8.4 |
| 15 | 1:40 | 7 | 3:20 | 12 | 2:17 | 10.4 |
| 16 | 3:00 | 13 | 0:42 | 3 | 0:19 | 1.5 |
| 17 | 8:00 | 33 | 9:54 | 36 | 8:09 | 37.2 |
| Total | 24:00 | 100 | 27:36 | 100 | 21:53 | 100.0 |

314 **Table 1.** Stage durations in hours and minutes along with %TED values for stages 1
315 to 17 of embryonic development in *D. melanogaster*, *M. abdita* and *M. scalaris*.

316

317 Comparison of embryonic stages and developmental events across the 3 species

318 indicates a number of features that contribute to the decreased developmental time

319 needed to go from egg to larva in *M. scalaris*. First, I find that the germband reaches

320 its maximum extent a stage earlier than in the other species and a consequence of

321 this heterochronic shift is that the germband is able to retract sooner. Additionally, I

322 find tightly coordinated movements of head involution and dorsal closure that are not

323 present in *M. abdita* and result in a compression of the time need to progress through

324 stages 9 to 13. A significantly compressed stage 16 in both *Megselia* species again

325 decreases the developmental time of *M. scalaris* over *D. melanogaster*. Finally,

326 heterochronic shifts in the stage at which the serosa ruptures and contracts results in

327 a reduction in time during which *M. scalaris* is enclosed in extraembryonic membrane.

328

329 **4. Conclusions**

330 In this paper I provide a detailed description of the embryonic development of the
331 coffin fly *M. scalaris*. In agreement with previous results, *M. scalaris* embryogenesis
332 is found to require less time to complete than *D. melanogaster*, and significantly less
333 time than the congener *M. abdita*. Comparison of stages across all 3 species reveals
334 heterochronic shifts, increased coordination of morphogenetic movements and
335 compression of individual stages all contribute to this rapid development.

336

337 **Acknowledgments**

338 I would like to thank Barbara Negre and Eva Jimenez-Guri for supplying *Megaselia*
339 *scalaris* and Eva Jimenez-Guri for help in troubleshooting the data. Additionally, I
340 would like to thank Eva Jimenez-Guri, Barbara Negre, Hilde Janssens and Yogi
341 Jaeger for feedback on the manuscript.

342

343 **References**

- 344 Campos-Ortega, J., Hartenstein, V., 1997. The Embryonic Development of
345 *Drosophila melanogaster* (2nd Edition), Springer, Heidelberg, DE. Springer,
346 Heidelberg, DE.
- 347 Disney, R.H.L., 2008. Natural history of the scuttle fly, *Megaselia scalaris*. Annu. Rev.
348 Entomol. 53, 39–60.
- 349 Foe, V.E., Alberts, B.M., 1983. Studies of nuclear and cytoplasmic behaviour during
350 the five mitotic cycles that precede gastrulation in *Drosophila* embryogenesis. J.
351 Cell Sci. 61, 31–70.
- 352 Jiménez-Guri, E., Huerta-Cepas, J., Cozzuto, L., Wotton, K.R., Kang, H.,
353 Himmelbauer, H., Roma, G., Gabaldón, T., Jaeger, J., 2013. Comparative
354 transcriptomics of early dipteran development. BMC Genomics 14, 123.
- 355 Jimenez-Guri, E., Wotton, K.R., Gavilán, B., Jaeger, J., Gavila, B., Jime, E., 2014. A
356 staging scheme for the development of the moth midge *Clogmia albipunctata*.
357 PLoS One 9, e84422.
- 358 Lemke, S., Stauber, M., Shaw, P.J., Rafiqi, A.M., Prell, A., Schmidt-Ott, U., 2008.
359 Bicoid occurrence and Bicoid-dependent hunchback regulation in lower
360 cyclorrhaphan flies. Evol. Dev. 10, 413–20.

- 361 Prawirodisastro, M., Benjamin, D., 1979. Laboratory study of the biology and ecology
362 of *Megaselia scalaris* (Diptera, Phoridae). *J. Med. Entomol.* 16, 317–20.
- 363 Rafiqi, A.M., Lemke, S., Ferguson, S., Stauber, M., Schmidt-Ott, U., 2008.
364 Evolutionary origin of the amnioserosa in cyclorrhaphan flies correlates with
365 spatial and temporal expression changes of zen. *Proc. Natl. Acad. Sci. U. S. A.*
366 105, 234–9.
- 367 Rafiqi, A.M., Lemke, S., Schmidt-ott, U., 2013a. The Scuttle Fly *Megaselia abdita* (
368 Phoridae): A Link between *Drosophila* and Mosquito Development Emerging
369 Model Organism The Scuttle Fly *Megaselia abdita* (Phoridae): A Link between
370 *Drosophila* and Mosquito Development.
- 371 Rafiqi, A.M., Lemke, S., Schmidt-ott, U., 2013b. *Megaselia abdita* : Fixing and
372 Devitellinizing Embryos Protocol *Megaselia abdita* : Fixing and Devitellinizing
373 Embryos 2011–2014.
- 374 Rafiqi, A.M., Lemke, S., Schmidt-ott, U., 2013c. *Megaselia abdita* : Preparing
375 Embryos for Injection Protocol *Megaselia abdita* : Preparing Embryos for
376 Injection 2011–2014.
- 377 Rasmussen, D.A., Noor, M.A.F., 2009. What can you do with 0.1x genome
378 coverage? A case study based on a genome survey of the scuttle fly *Megaselia*
379 *scalaris* (Phoridae). *BMC Genomics* 10, 382.
- 380 Sievert, V., Kuhn, S., Traut, W., 1997. Expression of the sex determining cascade
381 genes *Sex-lethal* and *doublesex* in the phorid fly *Megaselia scalaris*. *Genome*
382 40, 211–214.
- 383 Stauber, M., Jäckle, H., Schmidt-Ott, U., 1999. The anterior determinant *bicoid* of
384 *Drosophila* is a derived Hox class 3 gene. *Proc. Natl. Acad. Sci. U. S. A.* 96,
385 3786–9.
- 386 Stauber, M., Lemke, S., Schmidt-Ott, U., 2008. Expression and regulation of caudal
387 in the lower cyclorrhaphan fly *Megaselia*. *Dev. Genes Evol.* 218, 81–7.
- 388 Stauber, M., Taubert, H., Schmidt-Ott, U., 2000. Function of *bicoid* and *hunchback*
389 homologs in the basal cyclorrhaphan fly *Megaselia* (Phoridae). *Proc. Natl. Acad.*
390 *Sci. U. S. A.* 97, 10844–9.
- 391 Traut, W., 1994. Sex determination in the fly *Megaselia scalaris*, a model system for
392 primary steps of sex chromosome evolution. *Genetics* 136, 1097–1104.
- 393 Traut, W., 2010. New Y chromosomes and early stages of sex chromosome
394 differentiation: sex determination in *Megaselia*. *J. Genet.* 89, 307–313.
- 395 Varney, R., Noor, M., 2010. The scuttle fly. *Curr. Biol.* 20, 466–467.
- 396 Wiegmann, B.M., Trautwein, M.D., Winkler, I.S., Barr, N.B., Kim, J.-W., Lambkin, C.,
397 Bertone, M. a, Cassel, B.K., Bayless, K.M., Heimberg, A.M., Wheeler, B.M.,
398 Peterson, K.J., Pape, T., Sinclair, B.J., Skevington, J.H., Blagoderov, V.,
399 Caravas, J., Kutty, S.N., Schmidt-Ott, U., Kampmeier, G.E., Thompson, F.C.,
400 Grimaldi, D.A., Beckenbach, A.T., Courtney, G.W., Friedrich, M., Meier, R.,

- 401 Yeates, D.K., 2011. Episodic radiations in the fly tree of life. Proc. Natl. Acad.
402 Sci. U. S. A. 108, 5690–5.
- 403 Willhoeft, U., Traut, W., 1990. Molecular differentiation of the homomorphic sex
404 chromosomes in *Megaselia scalaris* (Diptera) detected by random DNA probes.
405 Chromosoma 99, 237–242.
- 406 Willhoeft, U., Traut, W., 1995. The sex-determining region of the *Megaselia scalaris*
407 (Diptera) Y chromosome. Chromosome Res. 3, 59–65.
- 408 Wotton, K.R., Crombach, A., Cicin-Sain, D., Ashyraliyev, M., Jaeger, J., 2012.
409 Efficient Reverse-Engineering of a Developmental Gene Regulatory Network.
410 PLoS Comput. Biol. 8, e1002589.
- 411 Wotton, K.R., Jiménez-Guri, E., García Matheu, B., Jaeger, J., Garcia Matheu, B.,
412 2014. A staging scheme for the development of the scuttle fly *Megaselia abdita*.
413 PLoS One 9, e84421.
- 414